Inorg. Chem. **2006**, *45*, 650–659

Homochiral and Heterochiral Coordination Polymers and Networks of Silver(I)

Tara J. Burchell and Richard J. Puddephatt*

Department of Chemistry, University of Western Ontario, London, Canada N6A 5B7

Received August 10, 2005

The self-assembly of racemic and enantiopure binaphthylbis(amidopyridyl) ligands 1,1′-$C_{20}H_{12}\{NHC(O)\text{-}4\text{-}C_5H_4N\}_2$, **1**, and 1,1′-$C_{20}H_{12}\{NHC(O)\text{-}3\text{-}C_5H_4N\}_2$, **2**, with silver(I) salts (AgX; X = CF_3CO_2, CF_3SO_3, NO_3) to form extended metal-containing arrays is described. It is shown that the self-assembly with racemic ligands can lead to homochiral or heterochiral polymers, through self-recognition or self-discrimination of the ligand units. The primary polymeric materials adopt helical conformations (secondary structure), and they undergo further self-assembly to form sheets or networks (tertiary structure). These secondary and tertiary structures are controlled through secondary bonding interactions between pairs of silver(I) centers, between silver cations and counteranions, or through hydrogen bonding involving amide NH groups. The self-assembly of the enantiopure ligand *R*-**1** with silver trifluoroacetate gave a remarkable three-dimensional chiral, knitted network composed of polymer chains in four different supramolecular isomeric forms.

Introduction

The coordination-driven self-assembly of metal−organic polymers, macrocycles, and networks based on a combination of metal−ligand coordination and secondary noncovalent interactions such as hydrogen bonding, electrostatic interactions, metal−metal contacts, and $\pi-\pi$ interactions is a major area of research,[1−4] and several groups have extended the approach to include the use of chiral ligands to control helicity.[5−8] For example, axially chiral functionalized 1,1′-binaphthyl units have been used as chiral building blocks

* To whom correspondence should be addressed. E-mail: pudd@uwo.ca. Fax: (519) 661-3022.

(1) (a) Steed, J. W.; Atwood, J. L. *Supramolecular Chemistry***;** VCH: New York, 2000. (b) Holliday, B. J.; Mirkin, C. A. *Angew. Chem., Int. Ed.* **2001**, *40*, 2022. (c) Sunatsuki, Y.; Motoda, Y.; Matsumoto, N. *Coord. Chem. Rev.* **2002**, *226*, 199. (d) Balamurugan, V.; Jacob, W.; Mukjerjee, J.; Mukherjee, R. *CrystEngComm* **2004**, 396. (e) Biradha, K. *CrystEngComm* **2003**, 374. (f) Beatty, A. M. *Coord. Chem. Rev.* **2003**, *246*, 131. (g) Roesky, H. W.; Andruh, M. *Coord. Chem. Rev.* **2003**, *236*, 91. (h) Kitagawa, S.; Kawata, S. *Coord. Chem. Rev.* **2002**, *224*, 11. (i) Tadokoro, M.; Nakasuji, K. *Coord. Chem. Rev.* **2000**, *198*, 205. (j) Conerney, B.; Jensen, P.; Kruger, P. E.; Moubaraki, B.; Murray, K. S. *CrystEngComm* **2003**, 454. (k) Albrecht, M. *Chem. Rev.* **2001**, *101*, 3457. (l) Aakeröy, C. B.; Desper, J.; Valdes-Martinez, J. *CrystEngComm.* **2004**, 413. (m) Badjic, J. D.; Nelson, A.; Cantrill, S. J.; Turnbull, W. B.; Stoddart, J. F. *Acc. Chem. Res.* **2005**, *38*, 723. (n) Hosseini, M. W. *Acc. Chem. Res.* **2005**, *38*, 313.

(2) (a) Muthu, S.; Yip, J. H. K.; Vittal, J. J. *J. Chem. Soc., Dalton Trans.* **2002**, 4561. (b) Muthu, S.; Yip, J. H. K.; Vittal, J. J. *J. Chem. Soc., Dalton Trans.* **2001**, 3577. (c) Schauer, C. L.; Matwey, E.; Fowler, F. W.; Lauher, J. W. *J. Am. Chem. Soc.* **1997**, *119*, 10245. (d) Aakeröy, C. B.; Beatty, A. M. *Chem. Commun.* **1998**, 1067. (e) Aakeröy, C. B.; Beatty, A. M.; Desper, J.; O'Shea, M.; Valdés-Martínez, J. *Dalton Trans.* **2003**, 3956. (f) Qin, Z.; Jennings, M. C.; Puddephatt, R. J. *Chem.*—Eur. J. **2002**, *8*, 735.

(3) (a) Qin, Z.; Jennings, M. C.; Puddephatt, R. J. *Inorg. Chem.* **2001**, *40*, 6220. (b) Qin, Z.; Jennings, M. C.; Puddephatt, R. J. *Chem. Commun.* **2001**, 2676. (c) Xu, X.; James, S. L.; Mingos, M. P.; White, A. J. P.; Williams, D. J.; *J. Chem. Soc., Dalton Trans.* **2000**, 3783. (d) Kuehl, C. J.; Tabellion, F. M.; Arif, A. M.; Stang, P. J. *Organometallics.* **2001**, *20*, 1956. (e) Li, G.; Song, Y.; Hou, H.; Li, L.; Fan, Y.; Zhu, Y.; Meng, X.; Mi, L. *Inorg. Chem.* **2003**, *42*, 913.

(4) (a) Burchell, T. J.; Eisler, D. J.; Jennings, M. C.; Puddephatt, R. J. *Chem. Commun.* **2003**, 2228. (b) Burchell, T. J.; Eisler, D. J.; Puddephatt, R. J. *Chem. Commun.* **2004**, 944. (c) Burchell, T. J.; Eisler, D. J.; Puddephatt, R. J. *Inorg. Chem.* **2004**, *43*, 5550.

(5) (a) Han, L.; Hong, M. *Inorg. Chem. Commun.* **2005**, *8*, 406. (b) Pschirer, N. G.; Ciurtin, D. M.; Smith, M. D.; Bunz, U. H. F.; zur Loye, H.-C. *Angew. Chem., Int. Ed.* **2002**, *41*, 583. (c) Ye, Q.; Wang, X.-S.; Zhao, H.; Xiong, R.-G. *Tetrahedron Asymmetry*, **2005**, *16*, 1595.

(6) (a) Telfer, S. G.; Kuroda, R. *Coord. Chem. Rev.* **2003**, *242*, 33. (b) Kesanli, B.; Lin, W. *Coord. Chem. Rev.* **2003**, *246*, 305.

(7) (a) Wu, C.-D.; Ngo, H. L.; Lin, W. *Chem. Commun.* **2004**, 1588. (b) Cui, Y.; Ngo, H. L.; White, P. S.; Lin, W. *Chem. Commun.* **2002**, 1666. (c) Cui, W.; Evans, O. R.; Ngo, H. L.; White, P. S.; Lin, W. *Angew. Chem., Int. Ed.* **2002**, *41*, 1159. (d) Evans, O. R.; Manke, D. R.; Lin, W. *Chem. Mater.* **2002**, *14*, 3866. (e) Cui, Y.; Lee, S. J.; Lin, W. *J. Am. Chem. Soc.* **2003**, *125*, 6014. (f) Ngo, H. L.; Lin, W. *J. Am. Chem. Soc.* **2002**, *124*, 14298. (g) Ngo, H. L.; Lin, W. *Chem. Commun.* **2003**, 1388. (h) Kesanli, B.; Cui, Y.; Smith, M. R.; Bittner, E. W.; Brockrath, B. C.; Lin, W. *Angew. Chem., Int. Ed.* **2004**, *44*, 72. (i) Lee, S. J.; Kim, J. S.; Lin, W. *Inorg. Chem.* **2004**, *43*, 6579. (j) Jiang, H.; Lin, W. *J. Am. Chem. Soc.* **2004**, *126*, 7426. (k) Lee, S. J.; Luman, C. R.; Castellano, F. N.; Lin, W. *Chem. Commun.* **2003**, *17*, 2124. (l) Jiang, H.; Lin, W. *J. Am. Chem. Soc.* **2003**, *125*, 8084. (m) Cui, Y.; Ngo, H. L.; White, P. S.; Lin, W. *Chem. Commun.* **2003**, *8*, 994. (n) Cui, Y.; Ngo, H. L.; White, P. S.; Lin, W. *Inorg. Chem.* **2003**, *42*, 652. (o) Cui, Y.; Ngo, H. L.; Lin, W. *Inorg. Chem.* **2002**, *41*, 5940.

10.1021/ic051365t CCC: $33.50
Published on Web 12/17/2005

for the self-assembly of chiral coordination complexes, which not only have interesting structures but may also have potential applications as functional molecular materials.[6−8] Elegant examples of homochiral metal-containing coordination complexes and networks prepared from enantiopure 1,1′-binaphthyl-derivatized ligands have been reported, including chiral coordination networks that have applications in enantioselective processes.[7]

Most previous studies have used enantiopure ligands, and so the materials formed are necessarily homochiral. A more complex and less explored situation arises when racemic ligands are used. Reactions with racemic ligands result in either ligand self-recognition whereby ligands of the same handedness associate to form a racemic mixture of homochiral complexes[6,7] or ligand self-discrimination whereby ligands of opposite handedness associate to form a heterochiral complex.[8a,9,10] When polymeric complexes are formed, the self-assembly with ligand self-recognition will give homochiral polymers, and the crystal will most commonly contain a racemic mixture, containing equal amounts of the *RRR*... and *SSS*... enantiomers. The solid state structures will then necessarily differ significantly from that of the homochiral polymer (*RRR*... or *SSS*... only) prepared from the enantiopure ligand.[4] The self-assembly can therefore be significantly different when using racemic versus enantiopure ligands, and there is great potential for discovering new and interesting solid-state architectures and molecular materials when the racemic ligands are used.

In the present research, both enantiopure and racemic forms of the binaphthylbis(amidopyridyl) ligands 1,1′-$C_{20}H_{12}$-{NHC(O)-4-C_5H_4N}$_2$, **1**, and 1,1′-$C_{20}H_{12}${NHC(O)-3-C_5H_4N}$_2$, **2** (Chart 1), were studied in self-assembly reactions with silver(I) salts AgX, with X = CF_3CO_2, CF_3SO_3, and NO_3. The aim was to determine if homochiral or heterochiral polymers might be obtained, as a function both of the ligand structure (**1** versus **2**) and of the coordinating strength of the anion. The incorporation of amido groups into the ligand backbone gives the potential for higher order self-assembly through hydrogen bonding, and there is also potential for self-assembly through argentophilic Ag···Ag interactions or through weak silver···anion bonding.[2−4] The binaphthylbis(amidopyridyl) ligands $C_{20}H_{12}${NHC(O)-4-C_5H_4N}$_2$, *rac*-**1**, and $C_{20}H_{12}${NHC(O)-3-C_5H_4N}$_2$, *rac*-**2** (Chart 1), have previously been shown to self-assemble through hydrogen bonding between N−H and pyridyl groups to form supramolecular polymers with chirality sequences [···*R*···*R*···*R*···, ···*S*···*S*···*S*···] and [···*R*···*S*···*R*···], respectively.[8a,c] In both ligands there is also an intramolecular hydrogen bond between an N−H and a C═O group of each molecule [**1**, N(2)···O(2) = 2.893(2) Å; **2**, N(2)···O(2) = 2.943(3) Å] that limits the span of the pyridyl donors [**1**, N(1)···N(4) = 9.97 Å; **2**, N(1)···N(4) = 6.61 Å] and controls the dihedral angle θ between the naphthyl groups (**1**, θ = 97.2°; **2**, 97.1°). In self-assembled coordination polymers which contain both labile metal−ligand bonds and other forms of dynamic bonding, there is an emerging consensus, based on the biological precedents, that the primary structure should be considered to be formed through the metal−ligand bonds, while secondary bonding forces such as hydrogen bonding, metallophilic bonding, π-stacking between aromatic groups, or weak interionic forces should be considered to control the secondary and tertiary structure, and the discussion below will adopt this approach.[1−8]

Chart 1. (a) Binaphthyl Ligands **1** and **2** and (b) Representation Showing the Conformation with Intramolecular Hydrogen Bond

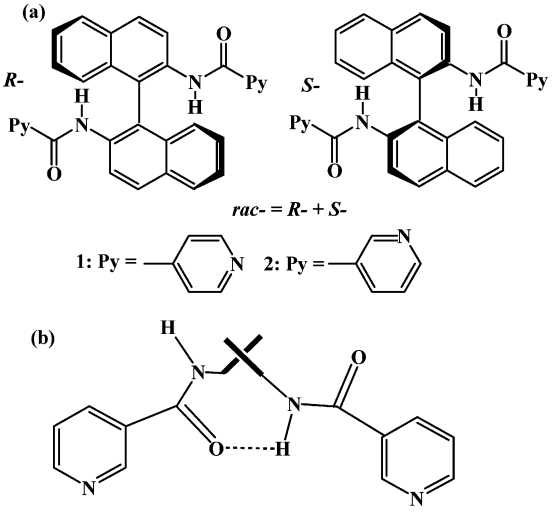

While metal−organic coordination compounds containing 1,1′-binaphthyl-derivatized ligands have been reported with metal centers such as Cu(II), Zn(II), Mn(II), Cd(II), Pt(II), Pd(II), and lanthanide metals,[7−10] the silver(I) compounds have not been studied extensively.[7a,8b] Most notably, homochiral lamellar silver(I) polymers of $AgNO_3$ or $AgClO_4$ and helical and double helical polymers of $AgNO_3$ were reported recently.[7a,8b]

Results

Polymeric Silver(I) Complexes with Ligands *rac*-1, *rac*-2, and *R*-1. Reaction of equimolar amounts of the binaphthylbis(amidopyridyl) ligands LL = *rac*-**1**, *rac*-**2**, or *R*-**1** with the silver(I) salts AgX gave the corresponding complexes [{(AgX)(μ-LL)}$_n$], **3a**−**4c** and **5a** (**3a**, LL = *rac*-**1**, X = CF_3CO_2; **3b**, LL = *rac*-**1**, X = CF_3SO_3; **3c**, LL = *rac*-**1**, X = NO_3; **4a**, LL = *rac*-**2**, X = CF_3CO_2; **4b**, LL = *rac*-**2**, X = CF_3SO_3; **4c**, LL = *rac*-**2**, X = NO_3; **5a**, LL = *R*-**1**, X = CF_3CO_2). The silver(I) complexes **3**−**5** were isolated as analytically pure, air-stable, white solids that slowly decomposed in solution or upon exposure to light. They are insoluble in most common organic solvents but soluble in DMSO and sparingly soluble in the mixed-solvent CH_2Cl_2−

(8) (a) Burchell, T. J.; Eisler, D. J.; Puddephatt, R. J. *Dalton Trans.* **2005**, 268. (b) Wang, R.; Xu, L.; Li, X.; Li, Y.; Shi, Q.; Zhou, Z.; Hong, M.; Chan, A. S. C. *Eur. J. Inorg. Chem.* **2004**, 1595. (c) Burchell, T. J.; Puddephatt, R. J. *Inorg. Chem.* **2005**, *44*, 3718.

(9) (a) Albrecht, M.; Schneider, M.; Röttele, H. *Angew. Chem., Int. Ed.* **1999**, *38*, 557. (b) Masood, M. A.; Enemark, E. J.; Stack, T. D. P. *Angew. Chem., Int. Ed.* **1998**, *37*, 928. (c) Krämer, R.; Lehn, J.-M.; Marquis-Rigault, A. *Proc. Natl. Acad. Sci. U.S.A.* **1993**, *90*, 5395. (d) Alkorta, I.; Elguero, J. *J. Am. Chem. Soc.* **2002**, *124*, 1488.

(10) (a) Kim, T. W.; Lah, M. S.; Hong, J.-I. *Chem. Commun.* **2001**, 743. (b) Hasenknopf, B.; Lehn, J.-M.; Baum, G.; Fenske, D. *Proc. Natl. Acad. Sci. U.S.A.* **1996**, *93*, 1397. (c) Zhou, X.-G.; Huang, J.-S.; Zhou, Z.-Y.; Cheung, K.-K.; Che, C.-M. *Inorg. Chim. Acta* **2002**, *331*, 194. (d) Claessens, C. G.; Torres, T. *J. Am. Chem. Soc.* **2002**, *124*, 14522.

Chart 2. Structure of Complex **3a** (X = CF_3CO_2): A Double-Stranded Polymer with Each Polymer Chain Homochiral

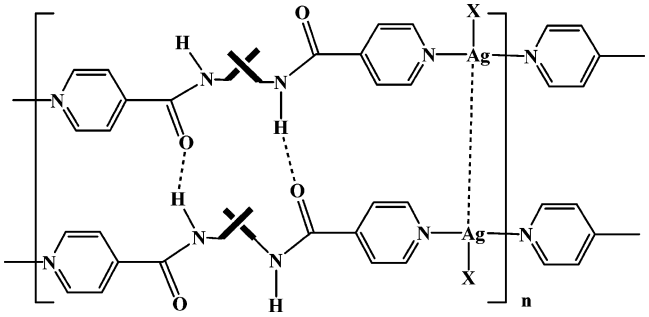

methanol. In the solid state, the complexes **3a**, **4a**−**c**, and **5a** will be shown to exist as polymers and they are soluble only in solvents that can break down the polymeric structures. A further complication is that all compounds crystallize as solvates. These solvate molecules can be guest molecules or they can play a significant role through weak coordination to silver(I) or by forming hydrogen bonds to amide NH groups of the ligands, but they are partially or fully lost on drying the solid samples.

The new complexes were characterized as dilute solutions in CH_2Cl_2−methanol by ESI mass spectrometry, and data below are reported for the ^{107}Ag isotope. The ESI-MS for the racemic complexes **3a**−**4c** were very similar to each other, with peaks at m/z = 495, 601, and 1095 corresponding to the fragments $[LL{\cdot}H]^+$, $[Ag{\cdot}LL]^+$, and $[Ag{\cdot}(LL)_2]^+$ (LL = *rac*-**1** or *rac*-**2**). In addition, the mass spectrum of complex **3a** contained a peak at m/z = 1201, corresponding to the fragment $[Ag_2{\cdot}(LL)_2(-H)]^+$ (LL = *rac*-**1**), and the spectra of complexes **4b**,**c** contained peaks at m/z = 1351 and 1264, corresponding to the similar fragment $[Ag_2{\cdot}(LL)_2(X)]^+$, where LL = *rac*-**2** and X = CF_3SO_3 and NO_3, respectively. The fragments are consistent with the complexes existing as either macrocycles or small oligomers in solution.

The ^{1}H NMR spectra of the complexes were obtained as solutions in DMSO-d_6, and details are given in the Experimental Section. The spectra showed resonances similar to, but shifted from, those of the free ligand. The spectra are consistent with the presence of macrocycles or with a dynamic equilibrium between macrocycles and oligomers. Unfortunately, the low solubility of the complexes in suitable solvents precluded a study by variable-temperature NMR. The structures of the complexes in solution are therefore not clearly defined, but it is clear that high polymers analogous to the solid-state structures described below are not present in solution.

Structure of Complex 3a, Formed from Ligand *rac*-1 with AgO_2CCF_3. The structure of complex **3a** in the solid state is depicted in Chart 2, in which the chiral binaphthyl groups are represented by bold crosses. The detailed structure is shown in Figure 1.

The structure of complex **3a** (as the solvate **3a**·0.7THF·0.3Et_2O) can be described as a one-dimensional polymer with silver trifluoroacetate groups bridged by the bis(pyridine) ligands. The stereochemistry at silver(I) is intermediate between T-shaped and trigonal, with the angle N(1)−Ag-

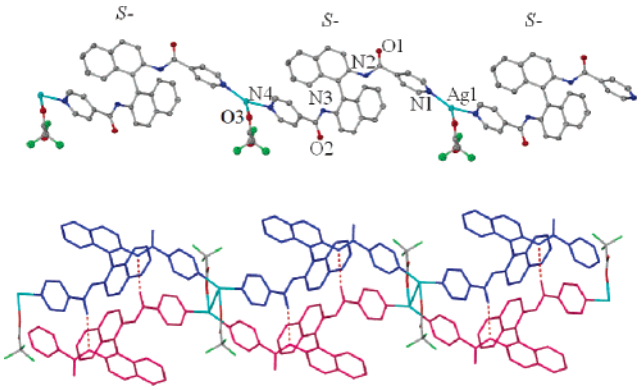

Figure 1. Views of the structure of complex **3a**. Top: Homochiral ...*SSS*... chain of **3a**. Bottom: Double-stranded polymer formed through Ag···Ag interactions and *R*···*S* amide hydrogen bonding between ...*RRR*... (pink) and ...*SSS*... (blue) chains. Selected bond parameters: Ag(1)−N(1) 2.212(5), Ag(1)−N(4A) 2.217(5), Ag(1)−O(3) 2.39(2), Ag(1)−Ag(1A) 3.357(1) Å; N(1)−Ag(1)−N(4A) 149.8(2), N(1)−Ag(1)−O(3) 102.6(5), N(4A)−Ag(1)−O(3) 105.1(5)°.

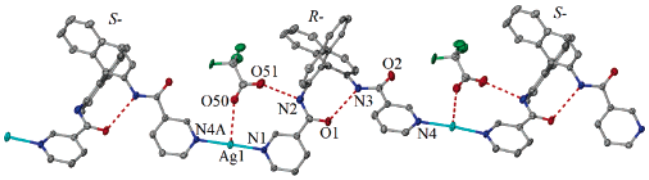

Figure 2. View of the structure of complex **4a**, showing the presence of a heterochiral polymer chain with intraligand N−H···O═C hydrogen bonds. Selected bond parameters: Ag(1)−N(1) 2.170(7), Ag(1)−N(4A) 2.181(6) Å; N(1)−Ag(1)−N(4A) = 171.9(3), N(1)−Ag(1)−Ag(1A) 97.3(2)°.

(1)−N(4A) = 149.8(2)°. The trifluoroacetate anions are clearly coordinated to silver, with Ag(1)−O(3) = 2.39(2) Å. Each polymer chain is homochiral with all binaphthyl groups having the same chirality *RRR* or *SSS*, and so the formula can be written as $[\{AgX(\mu\text{-}R\text{-}\mathbf{1})\}]_n$ or $[\{AgX(\mu\text{-}S\text{-}\mathbf{1})\}]_n$ with X = CF_3CO_2 (Figure 2, top). The conformations of the coordinated ligands in **3a** and the free ligand **1** are significantly different.[8c] The distance between nitrogen donor atoms of the pyridyl groups and the dihedral angle θ between the naphthyl groups are both larger in complex **3a** [N···N = 12.82 Å, θ = 109.2°] than in the free ligand **1** [N(1)···N(4) = 9.97 Å, θ = 97.2°],[8c] and there is an intramolecular NH···O═C hydrogen bond in the free ligand **1** but not in complex **3a**.

The most interesting feature of the structure of **3a** is that pairs of homochiral chains are further associated through secondary bonding interactions to form a double stranded polymer with one ...*RRR*... strand and one ...*SSS*... strand, as shown in Chart 2 and in Figure 1, bottom. These racemic double-stranded polymers are held together by interchain NH···O═C hydrogen bonds between amide groups [N···O = 2.840(6) Å] and by weak interchain Ag···Ag interactions [Ag···Ag = 3.357(1) Å]. In the hierarchy of the self-assembly process, the silver−ligand bonds are considered to give rise to the primary structure of the homochiral polymer chains, while the hydrogen bonding and argentophilic interactions control the secondary structure involving the double strand formation.

Chart 3. Structures of the Heterochiral Polymeric Complexes **4a**−**c**

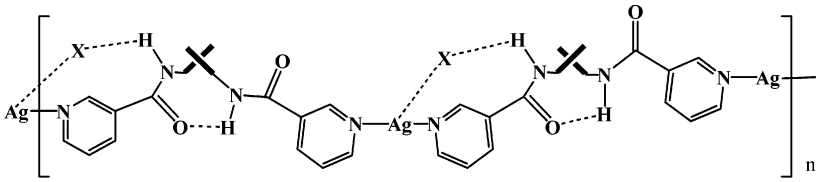

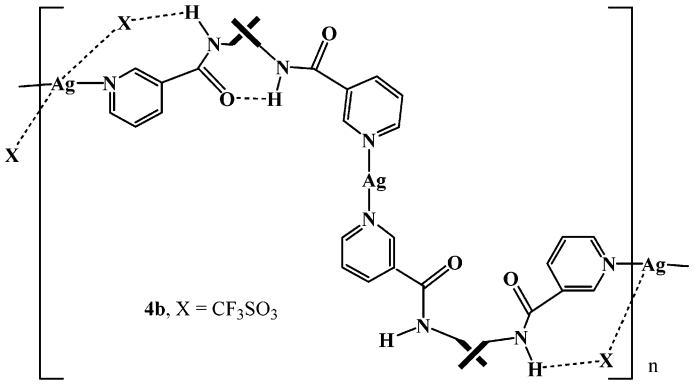

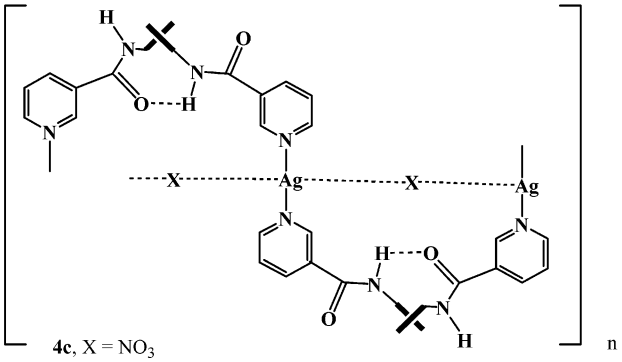

Structures of Complexes 4a−c, Formed from Ligand *rac*-2 with AgX (X = CF_3CO_2, CF_3SO_3, NO_3, Respectively). The structures of complexes **4a**−**c** are shown in Chart 3. In all cases the polymer chains are heterochiral, with the sequence [Ag(X)(*μ*-*R*-**2**)Ag(X)(*μ*-*S*-**2**)]$_n$, but there are significant differences in the conformations of the ligands **2**, in the binding of the anions, and in the nature of the interchain secondary bonding, as discussed below. The anion binding in complexes **4** is usually weak, and if the primary structure is considered to be the polymeric cation [Ag^+(*μ*-*R*-**2**)Ag^+-(*μ*-*S*-**2**)]$_n$, then complexes **4a**−**c** can be considered to contain different conformers of the polymer, with the secondary and tertiary structure determined in part by the cation−anion interactions.

The structure of complex **4a**, studied as the solvate **4a**·0.5THF·0.75 hexane, is depicted in Figures 2 and 3. In contrast to the homochiral polymeric complex **3a** (Figure 1), complex **4a** exists as a heterochiral polymer [Ag(X)(*μ*-*R*-**2**)Ag(X)(*μ*-*S*-**2**)]$_n$, in which there are equal numbers of *R* and *S* ligands in each polymer chain (Figure 2). Since both enantiomers of ligand **2** are present in complex **4a**, the polymer chain is more twisted than in **3a**. The trifluoroacetate anions are only weakly coordinated to the silver(I) centers (Ag···O = 2.69 Å) and the N−Ag−N angle deviates only slightly from linearity [N(1)−Ag−N(4) = 171.9(3)°], so the stereochemistry at silver is T-shaped. The trifluoroacetate anions are also weakly hydrogen bonded to an N−H group of the ligand [N(2)···O(51) = 2.71(1) Å]. The binaphthyl amide groups in the coordinated ligands of complex **4a** adopt

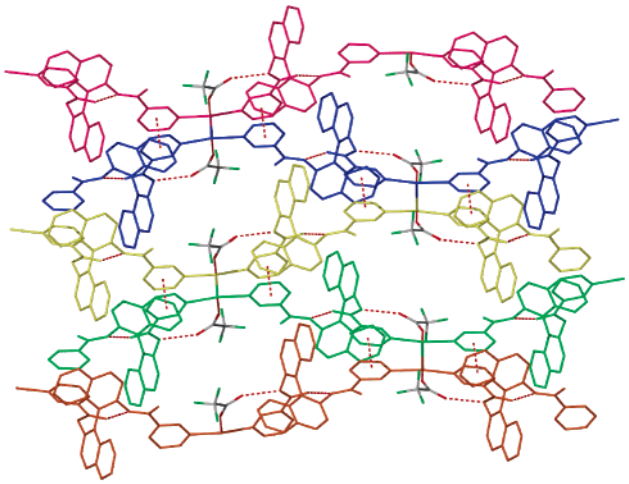

Figure 3. Two-dimensional sheet structure of complex **4a**. The sheet is formed by association of heterochiral polymer chains through intermolecular silver···silver secondary bonds [Ag(1)−Ag(1A) = 3.148(2) Å] and *π*−*π* interactions between pyridine groups.

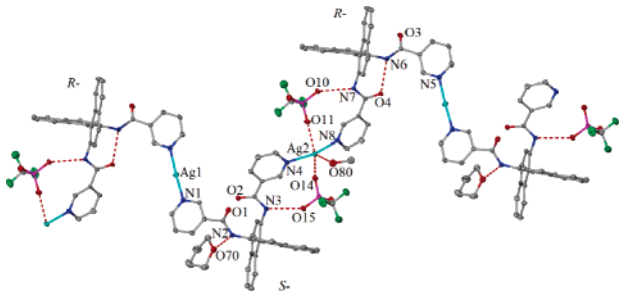

Figure 4. Solid-state structure of complex **4b**, showing the one-dimensional helical heterochiral polymer chain with weakly coordinated anions and methanol solvent molecules [coordinated through O(80)]. Selected bond parameters: Ag(1)−N(1) 2.147(4), Ag(1)−N(5) 2.153(4), Ag(2)−N(4A) 2.214(4), Ag(2)−N(8) 2.229(4) Å; N(1)−Ag(1)−N(5) 173.7(1), N(8)−Ag(2)−N(4A) 157.9(2)°.

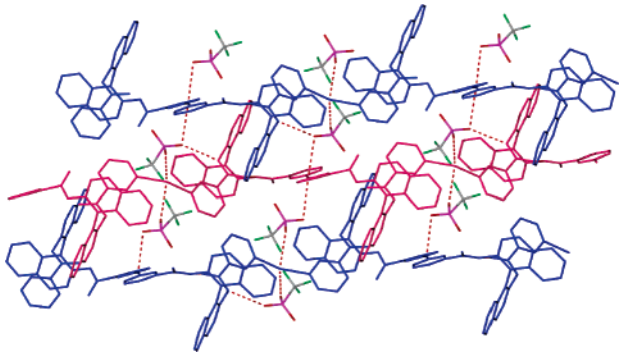

Figure 5. View of the two-dimensional sheet of complex **4b**. The sheet is formed through weak silver···anion···silver interactions.

a similar conformation as in the free ligand **2** (binaphthyl dihedral angle: **4a**, $\theta = 92.2°$; **2**, $\theta = 97.1°$] with a similar intramolecular N−H···O═C hydrogen bond [**4a**, N(3)···O(1) = 2.90(1) Å; **2**, N(2)···O(2) = 2.943(3) Å]. However, in complex **4a** the nitrogen atoms of the pyridyl groups are oriented in opposite directions and so the N···N separation is much longer in complex **4a** than in the free ligand **2** (**4a**, 10.3 Å; **2**, 6.61 Å).

The heterochiral polymer chains in **4a** are further associated through Ag···Ag interactions [Ag···Ag = 3.148(2) Å] and by aromatic $\pi-\pi$ stacking interactions between the associated pyridyl groups (centroid to centroid distance = 3.52 Å), as shown in Figure 3. The amide NH groups are involved in intrachain hydrogen bonding, either to the carbonyl group of an amide unit or to a trifluoroacetate ion, and so there is no interchain hydrogen bonding of the type observed for complex **3a**. Rather than forming a double-stranded polymer as in complex **3a**, each heterochiral polymer chain of complex **4a** associates with two other chains and so the interchain self-assembly leads to formation of a two-dimensional sheet structure. The sheets contain large open pores that are filled with THF solvent molecules of crystallization (not shown in Figure 3).

The structure of complex **4b**, studied as the solvate (**4b**)$_2$·THF·MeOH, is depicted in Chart 3 and in Figures 4 and 5. The complex exists as a helical, heterochiral polymer [Ag(X)(μ-*R*-**2**)Ag(X)(μ-*S*-**2**)]$_n$, X = triflate, with alternating right- and left-handed coils and a pitch of 20.7 Å (Figure 4). The *R* and *S* ligands in a given polymer chain of complex **4b** exist in two different conformations, labeled **I** and **II**. In conformation **I** there is an intraligand NH···O═C hydrogen bond [N(6)···O(4) = 2.794(5) Å]. However, in conformation **II**, the amidopyridyl arms are twisted such that both C═O groups face inward and both N−H groups face outward, and so there is no amide, amide NH···O═C hydrogen bond (Figure 4). There are corresponding differences in the N···N separation (**I**, N···N = 8.88 Å; **II**, 8.30 Å], the dihedral angle between the naphthyl groups (**I**, 93.4°; **II**, 84.7°), and the distances between the coordinated silver atoms (**I**, Ag···Ag = 10.34 Å; **II**, 10.58 Å] for the two ligand conformers. Each polymer chain contains both *R* and *S* ligands, but the individual chain is still chiral since the sequence is either [Ag(X)(μ-*R*-**2-I**)Ag(X)(μ-*S*-**2-II**)]$_n$ or its mirror image [Ag(X)(μ-*R*-**2-II**)Ag(X)(μ-*S*-**2-I**)]$_n$.

There are two different silver(I) centers in complex **4b**. One of them has an essentially linear N−Ag−N bond angle [N(1)−Ag(1)−N(5) = 173.7(1)°] and is 2-coordinate, while the other is distorted from linearity [N(4)−Ag(2)−N(8) = 157.9(2)°] and is also weakly coordinated to the oxygen atom of a methanol solvent molecule [Ag(2)···O(80) = 2.61 Å] and to two triflate anions [Ag(2)···O(11) = 2.68 Å, Ag(2)···O(14) = 2.84 Å] (Figure 4). If the secondary bonds are included, this silver(I) center could be considered to have distorted trigonal bipyramidal stereochemistry. The triflate ions also hydrogen bond to the adjacent NH groups [N(3)···O(15) = 2.905(5) Å, N(7)···O(10) = 2.841(5) Å], and so they form a bridge between the silver ions and the amide NH groups. The remaining amide NH group hydrogen bonds to a tetrahydrofuran solvent molecule [N(2)···O(7) = 2.906(5) Å]. The anions are also very weakly coordinated to the silver centers Ag(1) of neighboring polymer chains of opposite chirality [Ag(1)···O(10) = 3.09 Å, Ag(1)···O(15) = 3.10 Å], and these weak Ag···O interactions assemble individual polymer strands into two-dimensional sheets of polymers (Figure 5). There are no silver···silver interactions in complex **4b**.

The structure of complex **4c**, studied as the solvate (**4c**)$_2$·4CH_2Cl_2, is depicted in Chart 3 and in Figures 6 and 7 and can again be described as a helical heterochiral polymer [Ag(X)(μ-*R*-**2**)Ag(X)(μ-*S*-**2**)]$_n$, X = NO_3. The helical pitch is 13.7 Å. The coordinated ligands of complex **4c** exist in two slightly different conformations with similar dihedral angles (98.1, 94.7°), intramolecular N−H···O═C hydrogen bonds [N(3)···O(1) = 2.761(5) Å, N(6)···O(4) = 2.748(6) Å], and N···N separations [N(1)···N(4) = 6.85 Å, N(5)···N(8) = 7.06 Å]. The *R* and *S* ligands form right- and left-handed coils (Figure 6). The nitrate anions bridge between silver atoms through weak Ag···O bonds [Ag(1)···O(6) = 2.76 Å, Ag(1)···O(10) = 2.90 Å, Ag(2)···O(7) = 2.80 Å, Ag(2)···O(9) = 2.62 Å].

In complex **4c**, the association between polymer chains occurs by hydrogen bonding between the nitrate groups of one polymer chain and NH groups of neighboring polymer chains of opposite chirality [N(2)···O(9) = 3.156(8) Å, N(2)···O(10) = 2.954(6) Å, N(7)···O(5) = 2.842(7) Å], and thus, a two-dimensional sheet of polymers is formed (Figure

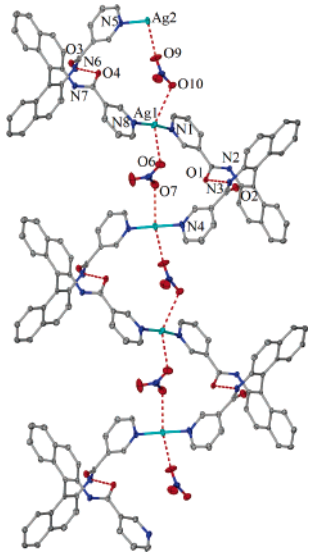

Figure 6. View of the structure of complex **4c**, showing a helical heterochiral polymer and the weak bonding interactions between the silver and nitrate ions. Selected bond parameters: Ag(1)−N(1) 2.165(5), Ag(1)−N(8A) 2.162(5), Ag(2)−N(4) 2.187(5), Ag(2)−N(5) 2.190(4) Å; N(1)−Ag(1)−N(8A) 172.0(2), N(4)−Ag(2)−N(5) 178.8(2)°.

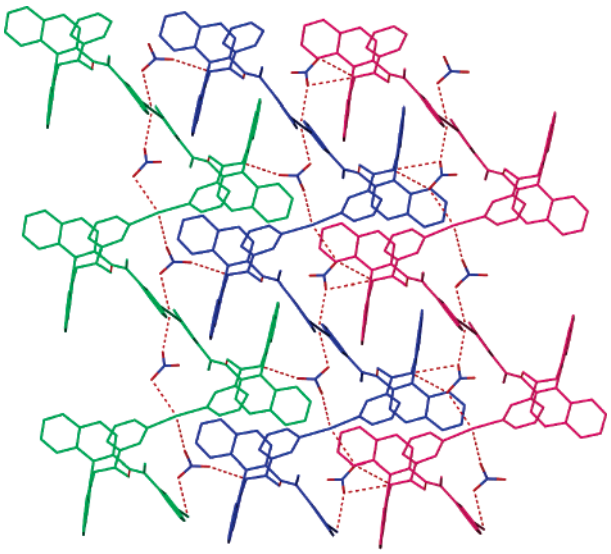

Figure 7. Two-dimensional sheet of polymers **4c**. The sheet is formed by linking chains through weak N−H···ONO_2 hydrogen-bonding interactions.

7). The solvate molecules occupy space between the sheets, but they do not take part in significant bonding interactions.

Structure of Complex 5a, Formed from Ligand *R*-1 with AgO_2CCF_3. The structure of the silver trifluoroacetate complex **5a**, studied as the solvate $(\mathbf{5a})_4 \cdot 5THF \cdot 3MeOH \cdot 2H_2O$, is particularly complex and is depicted in Chart 4 and in Figures 8−11, with selected bond distances and angles in Table 1. The structure of the enantiopure complex **5a** contains four independent polymers [labeled **5a(1)**−**5a(4)**; **5a(1)** contains silver atoms Ag(1), etc.], all of which contain $[Ag^+(\mu\text{-}R\text{-}\mathbf{1})\}]_n$ units and so can be considered as supramolecular isomers. The formula of **5a** is analogous to that of the *racemic* complex **3a**, but the structure is much more complex. In most polymeric complexes the chains pack parallel to one another, but complex **5a** forms an infinite

Chart 4. Schematic Structures of the "Supramolecular Isomers" of Polymeric Complex **5a** (X = CF_3CO_2)

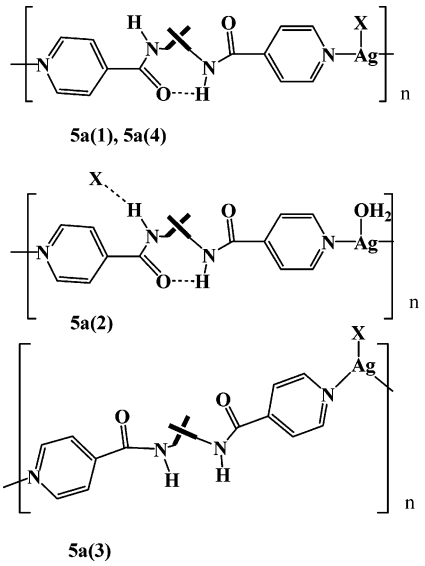

Table 1. Selected Bond Distances (Å) and Angles (deg) for Complex **5a**

		5a(1)	
Ag(1)−N(101)	2.170(8)	N(101)−Ag(1)−N(104A)	163.8(3)
Ag(1)−N(104A)	2.161(7)	N(101)−Ag(1)−O(451)	88.7(4)
Ag(1)−O(451)	2.599(10)	N(104A)−Ag(1)−O(451)	105.0(4)
		5a(2)	
Ag(2)−N(201)	2.177(7)	N(201)−Ag(2)−N(204B)	160.5(3)
Ag(2)−N(204B)	2.193(7)	N(201)−Ag(2)−O(21)	101.6(2)
Ag(2)−O(21)	2.547(7)	N(204B)−Ag(2)−O(21)	96.5(3)
		5a(3)	
Ag(3)−N(301)	2.277(8)	N(301)−Ag(3)−N(304C)	115.6(3)
Ag(3)−N(304C)	2.236(8)	N(301)−Ag(3)−O(350)	109.6(3)
Ag(3)−O(350)	2.331(10)	N(304A)−Ag(3)−O(350)	134.0(3)
		5a(4)	
Ag(4)−N(401)	2.155(8)	N(401)−Ag(4)−N(404D)	161.5(3)
Ag(4)−N(404D)	2.154(9)	N(401)−Ag(4)−O(450)	91.9(3)
Ag(4)−O(450)	2.510(9)	N(404D)−Ag(4)−O(450)	103.5(3)

knitted network in which the strands **5a(1)** propagate along the *c* axis, **5a(2)** along the *b* axis, and **5a(3)** and **5a(4)** along the *a* axis.

The structures of two of the polymer strands, **5a(1)** and **5a(2)**, are shown in Figure 8. Polymer strand **5a(1)** exists as a one-dimensional helical polymer with a pitch of 26.89 Å (Figure 8, top). The trifluoroacetate anions are weakly coordinated to the silver(I) centers [Ag(1)···O(451) =2.60-(1) Å], which have T-shaped stereochemistry. In strand **5a(1)** there is an intramolecular amide−amide hydrogen bond between an N−H and a C═O group of the ligands [N(103)···O(101) = 3.02(1) Å], the dihedral angle between the naphthyl rings in ligand *R*-**1** is 111.2°, and the distance between nitrogen atoms of the pyridyl rings is N(101)···N(104) = 11.49 Å. There is also a hydrogen-bonding interaction between an N−H group and the oxygen atom of a methanol molecule of crystallization [N(102)···O(75) = 2.96(1) Å] (not shown).

The polymer strand **5a(2)** is shown in Figure 8, bottom, and exists as a similar one-dimensional helical polymer with a pitch of 23.82 Å. The geometry of the ligands in strand

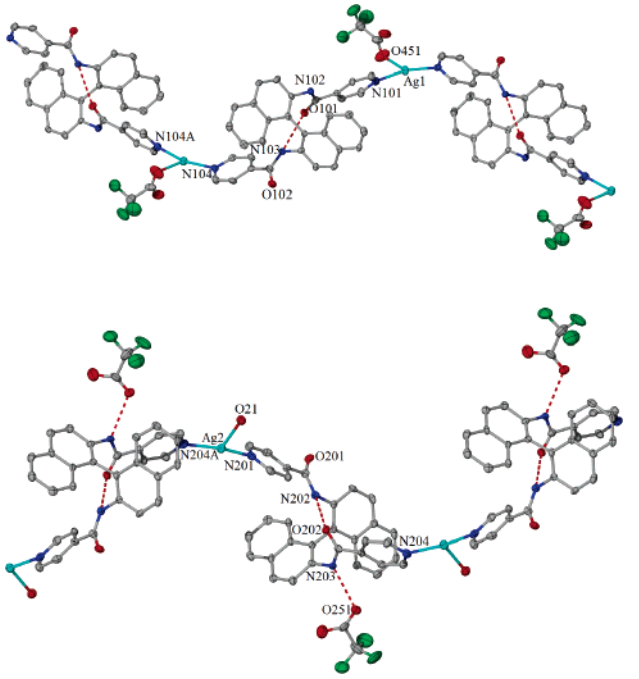

Figure 8. Structures of the polymer chains **5a(1)** and **5a(2)**. Top: View of chain **5a(1)** showing intramolecular N−H···O═C hydrogen bonding and coordination of anions to the silver centers. Bottom: View of chain **5a(2)** showing intramolecular N−H···O═C hydrogen bonding, N−H···O(trifluoroacetate) hydrogen bonding, and coordination of water to the silver centers.

5a(2) is similar to that of strand **5a(1)**, with a similar intramolecular amide hydrogen bond [N(202)···O(202) = 2.839(9) Å], bipyridyl bite distance [N(201)···N(204) = 10.06 Å], and torsion angle (112.7°). The silver(I) centers in strand **5a(2)** have T-shaped stereochemistry, but there is a water molecule coordinated to the silver atoms in place of the trifluoroacetate ligand in **5a(1)**, and the trifluoroacetate anions in strand **5a(2)** are hydrogen bonded to N−H groups of the ligands [N(203)···O(251) = 2.755(10) Å]. The strands **5a(1)** and **5a(2)** are isomers if the polymers are considered as the cations $[Ag^+(\mu\text{-}R\text{-}\mathbf{1})\}]_n$, but then they differ according to whether the anions or solvent molecules coordinate to silver(I) or form hydrogen bonds with amide NH groups.

The structures of polymer strands **5a(3)** and **5a(4)** are shown in Figure 9. Polymer strand **5a(4)** (Figure 9, top) is very similar to the polymer strands **5a(1)** and **5a(2)** and forms a helical polymer with a pitch of 23.50 Å. The ligands have a similar intramolecular amide hydrogen bond [N(403)···O(401) = 2.77(1) Å]. The angle between ligand naphthyl groups is 108.6°, and the distance between pyridyl nitrogen atoms is N(401)···N(404) = 9.74 Å. The trifluoroacetate anions are coordinated to the silver centers which have T-shaped coordination geometry [Ag(4)···O(450) = 2.510-(9) Å], as in strand **5a(1)**. This trifluoroacetate ion bridges between Ag(1) and Ag(4).

The structure of the polymer strand **5a(3)** (Figure 9, bottom) differs from the other strands with respect to both the coordination geometry of the metal center and the conformation of the ligand. Thus, in **5a(3)** the silver(I) centers adopt a trigonal rather than T-shaped coordination environment, with angle N(301)−Ag(3)−N(304) = 115.6-

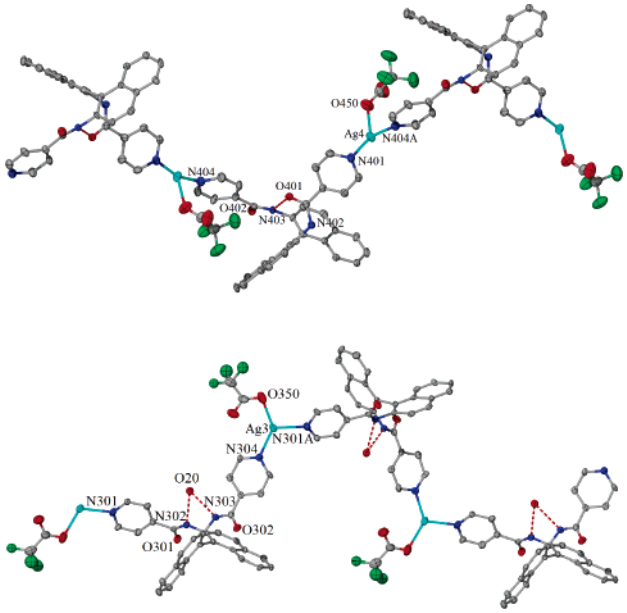

Figure 9. Solid-state structure of polymer chains **5a(3)** and **5a(4)** of complex **5a**. Top: View of chain **5a(4)** showing intramolecular N−H···O═C hydrogen bonding and coordination of anions to the silver centers. Bottom: View of chain **5a(3)** showing coordination of anions to the silver center and hydrogen bonding between N−H groups and water molecules.

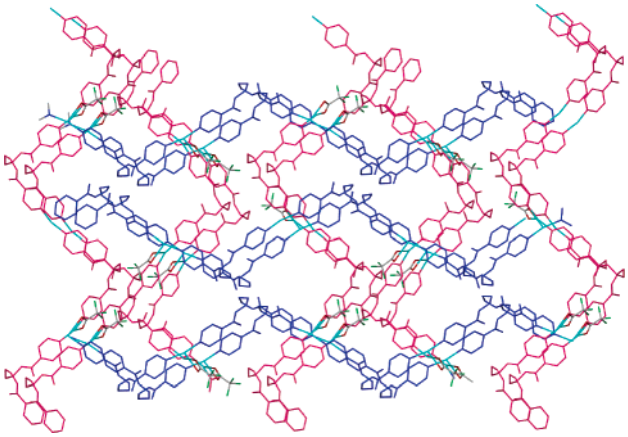

Figure 10. View down the *b*-axis of the three-dimensional chiral network of polymer chains **5a(1)** (blue, along *c*) and **5a(4)** (pink, along *a*) connected by bridging CF_3CO_2 anions. Only the backbone atoms of the binaphthyl groups are shown, and solvent molecules and other trifluoroacetate ions are omitted for clarity.

(3)°, as a result of the much stronger coordination of the trifluoroacetate group [Ag(3)−O(350) = 2.33(1) Å]. In addition, while the degree of rotation between the ligand naphthyl groups (107.8°) and distance between pyridyl nitrogen atoms [N(301)···N(304) = 11.56 Å] are similar to those of the other polymer strands, in **5a(3)** the amidopyridyl arms are rotated such that both N−H groups face inward and the C═O groups face outward, and thus, there are no intramolecular N−H···O═C hydrogen bonds. Instead, the N−H groups are hydrogen bonded to a water molecule [N(302)···O(20) = 2.952(9) Å, N(303)···O(20) = 3.000(9) Å] as shown in Figure 9, bottom.

Strands of polymers **5a(1)** and **5a(4)** are directly connected by bridging trifluoroacetate anions, and the helical polymers are therefore further assembled into a three-dimensional chiral silver(I) network (Figure 10).

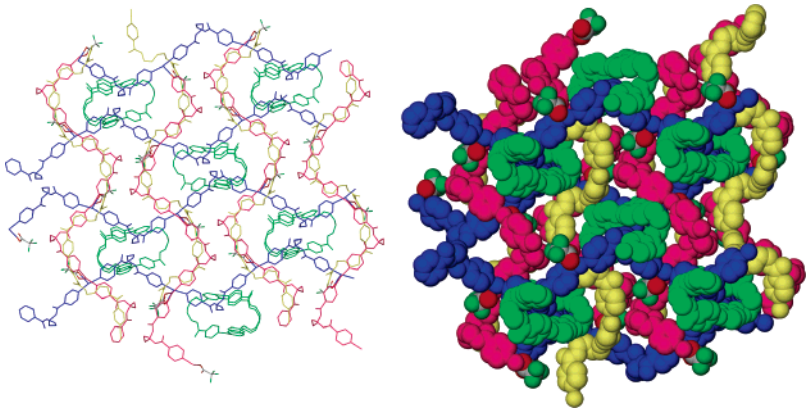

Figure 11. View down the *b*-axis of the overall structure of complex **5a**. The polymer strands **5a(2)** (green, along *b*) and **5a(3)** (yellow, along *a*) are threaded through the cavities of the three-dimensional chiral network of polymers **5a(1)** (blue, along c) and **5a(4)** (pink, along *a*). Naphthyl groups (except backbone atoms), solvent molecules, and most trifluoroacetate ions are omitted for clarity.

The network defined by the polymer chains **5a(1)** and **5a(4)** contains two types of large cavities, as shown in Figure 10, and the polymer strands **5a(2)** and **5a(3)** are threaded through the intricate chiral network as shown in Figure 11. The strands of **5a(3)**, which contain the kinked trigonal silver(I) centers, knit between strands of **5a(1)** by passing alternately above and below them. There is an indirect connection between the strands **5a(2)** and **5a(4)** through the sequence Ag(2)−O(21)(2.547(7) Å, water)···O(55)(2.70 Å, methanol)···N(402)(2.75 Å, amide).

Discussion

This work has developed the use of functionalized chiral 1,1′-binaphthyl ligands in the synthesis of unusual metal-containing complexes and networks.[6−8] The binaphthylbis(amidopyridyl) ligands have a natural helicity due to the restricted rotation about the C−C bond of the binaphthyl moiety, and so the complexes formed are helical in nature. The amidopyridyl groups impart additional helicity and flexibility to the ligands and allows them to adopt a range of conformations, which may be modified by the formation of an intramolecular hydrogen bond between an N−H and C═O group (Chart 1).[8c]

The helical shape of the binaphthylbis(amidopyridyl) ligands is well suited for polymer formation with metals that favor linear or slightly bent N−M−N bond angles, and all of the silver(I) complexes **3**−**5** crystallized as 1:1 polymers in the solid state. However, the primary and secondary structures of the polymers vary significantly with the ligand and anion. When the racemic binaphthylbis(amidopyridyl) ligands are used, the primary structure may contain homochiral polymers, as found in complex **3a** (Figure 1), or heterochiral polymers, as found in **4a**−**c** (Figures 2−7). This difference seems to be purely ligand dependent, with 4-pyridyl ligand *rac*-**1** giving the homochiral polymer **3a** and the 3-pyridyl ligand *rac*-**2** giving the heterochiral polymers **4a**−**c**.

The secondary structures of the polymers, considered as the conformations of individual polymer chains, appear to be determined primarily by hydrogen bonding, which in turn is affected by the nature of the anion and, in some cases, by the solvent. The homochiral polymeric complex **3a** does not contain an internal hydrogen bond of the type illustrated in Chart 1, but the heterochiral polymers **4a**,**c** do. In complex **4b**, only half of the ligands contain this internal hydrogen bond (Chart 3). The anions have a dominant effect in determining the secondary structures of complexes **4a**−**c**. In complex **4c**, the nitrate ions bridge between adjacent silver(I) centers and to span this distance the 3-pyridyl groups need to be oriented in a different way from that in **4a**,**b** to minimize the Ag···Ag separation (Chart 3). In complex **4a**, the trifluoroacetate ions coordinate weakly to silver(I) and also form a hydrogen bond to an amide NH group. In complex **4b**, a similar bridging of the triflate ions occurs (Chart 3) but alternate silver(I) centers contain either two or no such interactions. These anion effects, along with interactions of the polymer chains with solvent molecules in some cases, are subtle and could not readily be predicted.

The tertiary structure of the molecular materials, defined as the structure that results from interactions between polymer chains, can be controlled by hydrogen bonding, by argentophilic interactions, or by polar interactions with the anions. For example, the sheet structure of heterochiral complex **4a** arises from interchain Ag···Ag interactions only (Figure 3), whereas the double-stranded polymeric structure of the homochiral polymer **3a** arises through a combination of amide NH···O═C hydrogen bonds and Ag···Ag interactions (Figure 1). The two-dimensional sheet structure of complex **4b** arises through interchain ···silver···anion··· silver··· interactions (Figure 5). The different geometries of triflate and trifluoroacetate are probably responsible for the difference between the structures of **4b** (X = CF_3SO_3) and **4a** (X = CF_3CO_2), since an extra Ag···O interaction is present in **4b** in place of the Ag···Ag interaction in **4a**. The two-dimensional sheet structure of complex **4c** (Figure 7) arises through N−H···ONO_2 hydrogen bonding, involving the nitrate ions, which are also bridging between silver ions in individual polymer chains. Overall, the trioxo anions in **4b**,**c** each bridge between two silver(I) ions and also form a

Chart 5

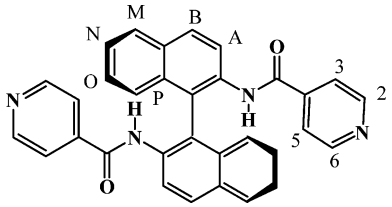

hydrogen bond to an NH group, but they differ significantly in the nature of intrachain and interchain components.

Complex **5a**, prepared from silver trifluoroacetate and the enantiopure ligand *R*-**1**, is remarkable in that four different one-dimensional polymer chains cocrystallize in the crystal lattice. Complexes composed of different polymeric topologies in the same crystal are unusual,[11] and we are unaware of any such chiral complexes prepared from a binaphthyl-derivatized ligand or of any case in which four different polymers are present. The four polymer chains of **5a** (Figures 8 and 9) may be considered to be supramolecular isomers, and the independent polymer chains in **5a** form a complex knitted network structure (Figures 10 and 11). The tertiary structure of this enantiopure complex **5a** is unique, and it is completely different from that of the analogous racemic complex **3a**.

At the onset of this research, we believed that the tertiary structures of these molecular materials would be determined by interchain hydrogen bonding between amide groups, of the form NH···O═C,[8c] but it transpired that this form of self-assembly was the exception rather than the rule. The amide NH groups were always involved in hydrogen bonding but often to the oxo anions and occasionally to solvent molecules instead of to amide C═O groups. Nevertheless, the main aim of the work, which was to determine if stereoselective self-assembly of polymers from racemic ligands could be effected, proved to be successful, along with a dramatic demonstration of the different structures that can arise from using racemic or enantiomerically pure chiral ligands.

Experimental Section

NMR spectra were recorded using a Varian Inova 400 NMR spectrometer. ^{1}H and ^{13}C chemical shifts are reported relative to tetramethylsilane (TMS). ESI mass spectra were recorded using a Micromass LCT spectrometer. The syntheses of ligands *rac*-**1**, *rac*-**2**, and *R*-**1** were described previously.[8a,8c] The ^{1}H NMR labeling diagram is shown below for ligand **1** (Chart 5).

The single crystals of the complexes reported below, used in X-ray structure determinations, incorporated solvent molecules, but the dried samples used for elemental analysis usually did not.

[{*μ*-*rac*-1,1′-$C_{20}H_{12}$-2,2′-(NHC(O)-4-$C_5H_4N)_2$}$_n$($AgCF_3CO_2$)$_n$], 3a. $AgCF_3CO_2$ (0.0662 g, 0.300 mmol) was added to a solution of *rac*-**1** (0.148 g, 0.300 mmol) in dichloromethane. After several minutes of stirring the complex precipitated out of solution as a white solid. The product was collected by filtration and dried under vacuum. Yield: 0.1512 g, 71%. NMR (DMSO-d_6; δ): 10.07 (s, 2H, NH), 8.57 (d, $^3J_{HH}$ = 5 Hz, 4H, $H^{2,6}$ py); 8.09 (d, $^3J_{HH}$ = 8 Hz, 2H, H^B); 7.98 (d, $^3J_{HH}$ = 8 Hz, 2H, H^M); 7.80 (d, $^3J_{HH}$ = 8 Hz, 2H, H^A); 7.45 (t, $^3J_{HH}$ = 8 Hz, 2H, H^N); 7.34 (d, $^3J_{HH}$ = 5 Hz, 4H, $H^{3,5}$ py); 7.28 (t, $^3J_{HH}$ = 8 Hz, 2H, H°); 6.97 (d, $^3J_{HH}$ = 8 Hz, 2H, H^P). Anal. Calcd for $C_{34}H_{18}N_4AgF_3O_4$: C, 57.4; H, 2.55; N, 7.88. Found: C, 57.35; H, 2.82; N, 7.29.

[{*μ*-*rac*-1,1′-$C_{20}H_{12}$-2,2′-(NHC(O)-3-$C_5H_4N)_2$}$_n$($AgCF_3CO_2$)$_n$], 4a. This was prepared similarly from $AgCF_3CO_2$ (0.0662 g, 0.300 mmol) and *rac*-**2** (0.148 g, 0.300 mmol). Yield: 0.1843 g, 86%. ^{1}H NMR (DMSO-d_6; δ): 10.01 (s, 2H, NH); 8.78 (d, $^3J_{HH}$ = 5 Hz, 2H, H^6 py); 8.57 (s, 2H, H^2 py); 8.12 (d, $^3J_{HH}$ = 9 Hz, 2H, H^B); 8.01 (d, $^3J_{HH}$ = 8 Hz, 2H, H^M); 7.85 (d, $^3J_{HH}$ = 9 Hz, 2H, H^A; d, $^3J_{HH}$ = 5 Hz, 2H, H^4 py); 7.47 (t, $^3J_{HH}$ = 8 Hz, 2H, H^N); 7.38 (dd, $^3J_{HH}$ = 5 Hz, 8 Hz, 2H, H^5 py); 7.31 (t, $^3J_{HH}$ = 8 Hz, 2H, H°); 7.02 (d, $^3J_{HH}$ = 8 Hz, 2H, H^P). Anal. Calcd for $C_{34}H_{18}N_4AgF_3O_4$: C, 57.4; H, 2.55; N, 7.88. Found: C, 57.48; H, 2.87; N, 7.50.

[{*μ*-*R*-1,1′-$C_{20}H_{12}$-2,2′-(NHC(O)-4-$C_5H_4N)_2$}$_n$($AgCF_3CO_2$)$_n$], 5a·1.25CH_2Cl_2. This was prepared similarly from $AgCF_3CO_2$ (0.0154 g, 0.070 mmol) and *R*-**1** (0.0345 g, 0.070 mmol). Yield: 0.0397 g, 79%. The NMR is the same as for **3a**. Anal. Calcd for $C_{34}H_{18}N_4AgF_3O_4$·1.25CH_2Cl_2: C, 51.53; H, 3.01; N, 6.82. Found: C, 51.79; H, 2.53; N, 6.87.

[{*μ*-*rac*-1,1′-$C_{20}H_{12}$-2,2′-(NHC(O)-4-$C_5H_4N)_2$}$_n$($AgCF_3SO_3$)$_n$], 3b. This was prepared similarly from $AgCF_3SO_3$ (0.0256 g, 0.100 mmol) and *rac*-**1** (0.0494 g, 0.100 mmol). Yield: 0.0493 g, 66%. NMR (DMSO-d_6; δ): 10.06 (s, 2H, NH), 8.57 (d, $^3J_{HH}$ = 5 Hz, 4H, $H^{2,6}$ py); 8.09 (d, $^3J_{HH}$ = 8 Hz, 2H, H^B); 7.98 (d, $^3J_{HH}$ = 8 Hz, 2H, H^M); 7.80 (d, $^3J_{HH}$ = 8 Hz, 2H, H^A); 7.46 (t, $^3J_{HH}$ = 8 Hz, 2H, H^N); 7.34 (d, $^3J_{HH}$ = 5 Hz, 4H, $H^{3,5}$ py); 7.28 (t, $^3J_{HH}$ = 8 Hz, 2H, H°); 6.97 (d, $^3J_{HH}$ = 8 Hz, 2H, H^P). Anal. Calcd for $C_{33}H_{22}N_4AgF_3O_5S$: C, 52.74; H, 2.95; N, 7.46. Found: C, 53.02; H, 2.70; N, 7.83.

[{*μ*-*rac*-1,1′-$C_{20}H_{12}$-2,2′-(NHC(O)-3-C_5H_4N)2}n($AgCF_3SO_3$)$_n$], 4b. This was prepared similarly from $AgCF_3SO_3$ (0.0256 g, 0.100 mmol) and *rac*-**2** (0.0494 g, 0.100 mmol). Yield: 0.0605 g, 80%. ^{1}H NMR (DMSO-d_6; δ): 10.01 (s, 2H, NH); 8.78 (d, $^3J_{HH}$ = 5 Hz, 2H, H^6 py); 8.57 (s, 2H, H^2 py); 8.12 (d, $^3J_{HH}$ = 9 Hz, 2H, H^B); 8.00 (d, $^3J_{HH}$ = 8 Hz, 2H, H^M); 7.85 (d, $^3J_{HH}$ = 9 Hz, 2H, H^A; d, $^3J_{HH}$ = 5 Hz, 2H, H^4 py); 7.47 (t, $^3J_{HH}$ = 8 Hz, 2H, H^N); 7.38 (dd, $^3J_{HH}$ = 5 Hz, 8 Hz, 2H, H^5 py); 7.31 (t, $^3J_{HH}$ = 8 Hz, 2H, H°); 7.02 (d, $^3J_{HH}$ = 8 Hz, 2H, H^P). Anal. Calcd for $C_{33}H_{22}N_4AgF_3O_5S$: C, 52.74; H, 2.95; N, 7.46. Found: C, 52.76; H, 2.59; N, 7.34.

[{*μ*-*rac*-1,1′-$C_{20}H_{12}$-2,2′-(NHC(O)-4-$C_5H_4N)_2$}$_n$($AgNO_3$)$_n$], 3c. This was prepared similarly from an acetonitrile solution of $AgNO_3$ (0.0169 g, 0.100 mmol) and *rac*-**1** (0.0494 g, 0.100 mmol). Yield: 0.0469 g, 71%. NMR (DMSO-d_6; d): 10.07 (s, 2H, NH), 8.56 (d, $^3J_{HH}$ = 5 Hz, 4H, $H^{2,6}$ py); 8.09 (d, $^3J_{HH}$ = 8 Hz, 2H, H^B); 7.97 (d, $^3J_{HH}$ = 8 Hz, 2H, H^M); 7.80 (d, $^3J_{HH}$ = 8 Hz, 2H, H^A); 7.45 (t, $^3J_{HH}$ = 8 Hz, 2H, H^N); 7.34 (d, $^3J_{HH}$ = 5 Hz, 4H, $H^{3,5}$ py); 7.27 (t, $^3J_{HH}$ = 8 Hz, 2H, H°); 6.97 (d, $^3J_{HH}$ = 8 Hz, 2H, H^P). Anal. Calcd for $C_{32}H_{22}AgN_5O_5$: C, 57.85; H, 3.34; N, 10.54. Found: C, 57.43; H, 3.14; N, 10.17.

[{*μ*-*rac*-1,1′-$C_{20}H_{12}$-2,2′-(NHC(O)-3-$C_5H_4N)_2$}$_n$($AgNO_3$)$_n$], 4c. This was prepared similarly from an acetonitrile solution of $AgNO_3$ (0.0169 g, 0.100 mmol) and *rac*-**2** (0.0494 g, 0.100 mmol). Yield: 0.0565 g, 85%. ^{1}H NMR (DMSO-d_6; δ): 10.02 (s, 2H, NH); 8.79 (d, $^3J_{HH}$ = 5 Hz, 2H, H^6 py); 8.57 (s, 2H, H^2 py); 8.12 (d, $^3J_{HH}$ = 9 Hz, 2H, H^B); 8.01 (d, $^3J_{HH}$ = 8 Hz, 2H, H^M); 7.85 (d, $^3J_{HH}$ = 9

(11) (a) Carlucci, L.; Ciani, G.; Moret, M.; Proserpio, D. M.; Rizzato, S. *Angew. Chem., Int. Ed.* **2000**, *39*, 1506. (b) Itaru, S.; Kadowaki, K.; Soai, K. *Angew. Chem., Int. Ed.* **2000**, *39*, 1510. (c) Yang, W.; Zhang, J.; Li, Z.-J.; Gao, S.; Kang, Y.; Chen, Y.-B.; Wen, Y.-H.; Yao, Y.-G. *Inorg. Chem.* **2004**, *43*, 6525. (d) Jiang, Y.-C.; Lai, Y.-C.; Wang, S.-L.; Lii, K.-H. *Inorg. Chem.* **2001**, *40*, 5320. (e) Ayyappan, P.; Evans. O. R.; Lin, W. *Inorg. Chem.* **2002**, *41*, 3329. (f) Biradha, K.; Fujita, M. *Chem. Commun.* **2002**, 1866. (g) Carlucci, L.; Ciani, G.; Proserpio, D. M. *Chem. Commun.* **2004**, 380.

Table 2. Crystallographic Data for Solvated Complexes **3a**, **4a**−**c**, and **5a**

param	**3a**·0.7THF·0.3Et_2O	**4a**·0.5THF·0.75hexane	(**4b**)$_2$·THF·MeOH	(**4c**)$_2$·4CH_2Cl_2	(**5a**)$_4$·5THF·3MeOH)·2H_2O
formula	$C_{38}H_{30.6}AgF_3N_4O_5$	$C_{40.5}H_{36.5}AgF_3N_4O_{4.5}$	$C_{71}H_{56}Ag_2F_6N_8O_{12}S_2$	$C_{68}H_{52}Ag_2Cl_8N_{10}O_{10}$	$C_{159}H_{144}Ag_4F_{12}N_{16}O_{26}$
fw	788.13	816.11	1607.10	1668.54	3354.38
space group	*C*2/*c*	$P2_1/n$	$P\bar{1}$	$P\bar{1}$	$P2_12_12_1$
a (Å)	30.263(6)	14.291(3)	13.882(3)	13.459(3)	23.500(5)
b (Å)	13.942(3)	10.937(2)	13.959(3)	13.672(3)	23.828(5)
c (Å)	16.903(3)	24.711(5)	19.119(4)	19.467(4)	26.897(5)
α (deg)	90	90	99.13(3)	97.74(3)	90
β (deg)	109.96(3)	92.77(3)	103.92(3)	106.86(3)	90
γ (deg)	90	90	105.97(3)	94.18(3)	90
T (K)	150	150	150	150	150
λ (Å)	0.710 73	0.710 73	0.710 73	0.710 73	0.710 73
V (Å^3)	6703(2)	3857.9(13)	3355.3(12)	3373.2(12)	1506.1(5)
Z	8	4	2	2	4
D_{calc} (Mg/m^3)	1.562	1.405	1.591	1.643	1.479
μ (mm^{-1})	0.670	0.583	0.733	0.965	0.604
R1, wR2 [$I > 2\sigma(I)$]	0.0622, 0.1379	0.0838, 0.2192	0.528, 0.1185	0.0682, 0.1788	0.0636, 0.1469
R indices (all data)	0.1208, 0.1634	0.1583, 0.2504	0.0821, 0.1325	0.1006, 0.2001	0.1696, 0.1858

Hz, 2H, H^A; d, $^3J_{HH}$ = 5 Hz, 2H, H^4 py); 7.46 (t, $^3J_{HH}$ = 8 Hz, 2H, H^N); 7.38 (dd, $^3J_{HH}$ = 5 Hz, 8 Hz, 2H, H^5 py); 7.31 (t, $^3J_{HH}$ = 8 Hz, 2H, H°); 7.02 (d, $^3J_{HH}$ = 8 Hz, 2H, H^P). Anal. Calcd for $C_{32}H_{22}AgN_5O_5$: C, 57.85; H, 3.34; N, 10.54. Found: C, 57.69; H, 3.17; N, 10.14.

X-ray Structure Determinations. A crystal suitable for X-ray analysis was mounted on a glass fiber. Data were collected at 150 K using a Nonius-Kappa CCD diffractometer using COLLECT (Nonius, BV, 1998) software. The unit cell parameters were calculated and refined from the full data set. Crystal cell refinement and data reduction was carried out using the Nonius DENZO package. The data were scaled using SCALEPACK (Nonius, BV, 1998). The SHELX-TL V5.1 and SHELX-TL V6.1 (G. M. Sheldrick) program packages were used to solve and refine the structures. The structures of complexes **3a**, **4c**, and **5a** were solved by direct methods, while the structures of complexes **4a**,**b** were solved by the automated Patterson routine of the SHELX-TL software package. Except as mentioned, all non-hydrogen atoms were refined with anisotropic thermal parameters. The hydrogen atoms were calculated geometrically and were riding on their respective carbon atoms. Crystal data are summarized in Table 2. All thermal ellipsoid diagrams are shown at 30% probability.

3a·0.7THF·0.3Et_2O. Crystals of *rac*-(±)-[$C_{34}H_{22}AgF_3N_4O_4$]·0.7THF·0.3Et_2O were grown from diffusion of ether into a THF−methanol solution of the complex. The trifluoroacetate group was partially disordered: the O3 atom was modeled as a 50:25:25 isotropic mixture, and the F_3 moiety was modeled as a 40:40:20 isotropic mixture. The solvent was disordered and was modeled isotropically as a 70:15:15 THF−ether−ether mixture with geometric restraints. The largest residual electron density peak (0.527 e/Å^3) was associated with one of the fluorine atoms.

4a·0.5THF·0.75hexane. Crystals of *rac*-(±)-[$C_{34}H_{22}AgF_3N_4O_4$]·0.5THF·0.75hexane were grown from diffusion of hexane into a THF−methanol solution of the complex. The trifluoroacetate group was disordered and modeled as a (50:50) mixture. All of the solvent molecules were refined isotropically, and the THF solvent molecule and one of the hexane solvent molecules were each refined at 50% occupancy with geometric restraints. The hexane solvent molecules were situated on a symmetry element. The largest residual electron density peak (0.808 e/Å^3) was associated with one of the solvent molecules.

(4b)$_2$·THF·MeOH. Crystals of *rac*-(±)-[$C_{66}H_{44}Ag_2F_6N_8O_{10}S_2$]·THF·MeOH were grown from diffusion of hexane into a THF−methanol solution of the complex. The methanol solvent molecule was refined as a 65:30 isotropic mixture. The largest residual electron density peak (0.950 e/Å^3) was associated with one of the silver atoms.

(4c)$_2$·4CH_2Cl_2. Crystals of [$C_{64}H_{42}Ag_2N_{10}O_{10}$]·4$CH_2Cl_2$ were grown from diffusion of hexane into a CH_2Cl_2−methanol−acetonitrile solution of the complex. All non-hydrogen atoms were refined with anisotropic thermal parameters. The largest residual electron density peak (3.606 e/Å^3) was associated with one of the silver atoms.

(5a)$_4$·5THF·3MeOH·2H_2O. Crystals of (*R*)-(+)-[$C_{136}H_{88}Ag_4F_{12}N_{16}O_{16}$]·5THF·3MeOH·2$H_2O$ were grown from diffusion of hexane into a THF−methanol solution of the complex. One of the CF_3 groups was disordered and was refined as a 55:45 isotropic mixture with geometric restraints. All of the THF and methanol solvent molecules were refined isotropically, and two of the THF molecules were refined at 50% occupancy. The Flack parameter refined to a value of 0.00(2) indicating the correct hand of the molecule was refined. The largest residual electron density peak (1.045 e/Å^3) was associated with one of the solvent molecules.

Acknowledgment. We thank the NSERC (Canada) for financial support and for a scholarship to T.J.B. R.J.P. thanks the Government of Canada for a Canada Research Chair.

Supporting Information Available: X-ray crystallographic data in cif format. This material is available free of charge via the Internet at http://pubs.acs.org.

IC051365T